Improved Diagnosis of Viable Parenchymal Neurocysticercosis by Combining Antibody Banding Patterns on Enzyme-Linked Immunoelectrotransfer Blot (EITB) with Antigen Enzyme-Linked Immunosorbent Assay (ELISA)

Gianfranco Arroyo,[a,b] Javier A. Bustos,[a,b] Andres G. Lescano,[a] Isidro Gonzales,[b] Herbert Saavedra,[b] E. Javier Pretell,[c] Yesenia Castillo,[a] Erika Perez,[b] Pierre Dorny,[d] Robert H. Gilman,[e] Seth E. O'Neal,[a,f] Armando E. Gonzalez,[g] Hector H. Garcia,[a,b] for the Cysticercosis Working Group in Peru (CWGP)

[a]Center for Global Health, Universidad Peruana Cayetano Heredia, Lima, Peru
[b]Cysticercosis Unit, Instituto Nacional de Ciencias Neurologicas, Lima, Peru
[c]Department of Neurology, Hospital Nacional Alberto Sabogal, Callao, Peru
[d]Department of Biomedical Sciences, Institute of Tropical Medicine, Antwerp, Belgium
[e]Department of International Health, Bloomberg School of Public Health, Johns Hopkins University, Baltimore, Maryland, USA
[f]School of Public Health, Oregon Health & Science University-Portland State University, Portland, Oregon, USA
[g]School of Veterinary Medicine, Universidad Nacional Mayor de San Marcos, Lima, Peru

ABSTRACT The diagnosis of neurocysticercosis (NCC) depends on neuroimaging and serological confirmation. While antibody detection by enzyme-linked immunoelectrotransfer blot (EITB) fails to predict viable NCC, EITB banding patterns provide information about the host's infection course. Adding antigen enzyme-linked immunosorbent assay (Ag-ELISA) results to EITB banding patterns may improve their ability to predict or rule out of viable NCC. We assessed whether combining EITB banding patterns with Ag-ELISA improves discrimination of viable infection in imaging-confirmed parenchymal NCC. EITB banding patterns were grouped into classes using latent class analysis. True-positive and false-negative Ag-ELISA results in each class were compared using Fisher's exact test. Four classes were identified: 1, EITB negative or positive to GP50 alone (GP50 antigen family); 2, positive to GP42-39 and GP24 (T24/42 family), with or without GP50; and 3 and 4, positive to GP50, GP42-39, and GP24 and reacting to bands in the 8-kDa family. Most cases in classes 3 and 4 had viable NCC (82% and 88%, respectively) compared to classes 2 and 1 (53% and 5%, respectively). Adding positive Ag-ELISA results to class 2 predicted all viable NCC cases (22/22 [100%]), whereas 11/40 patients (27.5%) Ag-ELISA negative had viable NCC ($P < 0.001$). Only 1/4 patients (25%) Ag-ELISA positive in class 1 had viable NCC, whereas 1/36 patients (2.8%) Ag-ELISA negative had viable NCC ($P = 0.192$). In classes 3 and 4, adding Ag-ELISA was not contributory. Combining Ag-ELISA with EITB banding patterns improves discrimination of viable from nonviable NCC, particularly for class 2 responses. Together, these complement neuroimaging more appropriately for the diagnosis of viable NCC.

KEYWORDS Ag-ELISA, EITB banding patterns, *Taenia solium*, viable NCC

Neurocysticercosis (NCC) is an infection of the human central nervous system (CNS) with larvae of the "pork tapeworm" *Taenia solium* (1, 2). NCC is the leading cause of secondary epilepsy worldwide and is endemic in poor rural areas lacking sanitation and where pigs free roam for food (2, 3). NCC is also an emerging disease in developed countries due to migration of cases from areas of endemicity (4, 5). NCC is on the list of neglected tropical diseases worldwide (6) and produces a negative impact on public health due to late

diagnosis resulting from its slow disease progression, as well as the associated economic burden due to treatment costs, disability, and productivity losses (5, 7).

Symptoms in NCC depend on the characteristics of the CNS cyst infection (location, developmental stage, and number) and the host's immune response (8, 9). Epilepsy is the most frequent neurological manifestation and is mainly associated with parenchymal brain cysts (9–11). Brain cysts may remain silent for a long period of time, until the parasite is recognized by the host's immune system, thereby triggering an inflammatory response, leading to cyst degeneration and, in some cases, development of residual calcifications that can persist as epileptogenic foci (12, 13). Antiparasitic treatment accelerates the process of cyst degeneration, cyst death, and resolution, which in turns produces a beneficial clinical effect in patients (14–16).

Neuroimaging constitutes the main diagnostic tool for NCC, allowing recognition of CNS cysts, their location, developmental phase, and number (17). Magnetic resonance (MR) is highly sensitive in detecting viable cysts, although its sensitivity for residual calcifications is lower (18, 19). Computed tomography (CT) is superior in detecting calcified lesions (20, 21). Imaging findings are not always definitive, and in some cases, neuroimaging fails to detect CNS lesions. Serological assays can support or refute the diagnosis of NCC, particularly when neuroimaging is not conclusive (22).

The enzyme-linked immunoelectrotransfer blot (EITB) assay is the reference serological test for antibody detection in NCC, and it recognizes antibody bands to seven parasite glycoproteins (GP50, GP42-39, GP24, GP21, GP18, GP14, and GP13) (23). EITB is highly sensitive and specific (98% and 100%) in patients with multiple viable NCC cysts, although its sensitivity to detect single viable lesions is lower (24). Antibody responses demonstrate exposure but not necessarily active infection, as antibodies may persist after cyst resolution. While an overall positive or negative categorization of EITB results fails to predict viable infection (25), antibody profiles on EITB are not random (26, 27); the band distribution reflects the presence or absence of three distinct antigen families in *T. solium* that differ in structure and function. The GP50 family includes glycosylated and glycosylphosphatidylinositol (GPI)-anchored membrane proteins that migrate at the position of 50 kDa (28). The T24/42 antigen family includes tetraspanins (membrane-spanning proteins) that migrate at positions of 42 kDa and at homodimers of 24 kDa on EITB (29). The 8-kDa antigen family includes small proteins found at 21, 18, 14, and 13 kDa on EITB, and they have been characterized as parasite excretory-secretory products with probable immune evasion activity (30, 31). EITB antibody banding patterns can provide useful information as their distribution is associated with imaging findings in NCC. Negative or weak antibody responses (to GP50 only) are associated with nonviable NCC, whereas antibody responses involving low-molecular-weight antigens (related to the 8-kDa antigen family) are strongly associated with extraparenchymal NCC or multiple parenchymal cysts (26, 27).

Antigen detection indicates the presence of viable cysts and also provides information about cyst burden and severity of infection (27). The development of monoclonal antibody (MAb)-based antigen enzyme-linked immunosorbent assays (Ag-ELISAs) greatly improved the use of antigen detection for diagnosis of viable NCC (25). However, the sensitivity of current Ag-ELISAs is lower than that of EITB and is strongly affected by the number of viable lesions (25, 32). Considering Ag-ELISA in addition to EITB banding patterns may improve discrimination of viable from nonviable CNS cyst infections, and together they may complement more appropriately neuroimaging in defining infection status with viable cysts in NCC. Therefore, this study aimed to assess the combined use of EITB banding patterns with Ag-ELISA for viable parenchymal NCC.

MATERIALS AND METHODS

Study design and participants. This study is a cross-sectional study of all symptomatic patients attending the Cysticercosis Unit at the Instituto Nacional de Ciencias Neurologicas (INCN) in Lima, Peru, for initial diagnosis of NCC (from 2015 to 2019). Patients were initially eligible if they had a brain MRI and CT scan taken within a window period of 3 months after or before their first diagnostic serum sample to avoid a bias effect on disease progression between neuroimaging and serology (Fig. 1). Patients were subsequently included if they had lesions compatible with parenchymal NCC on neuroimages:
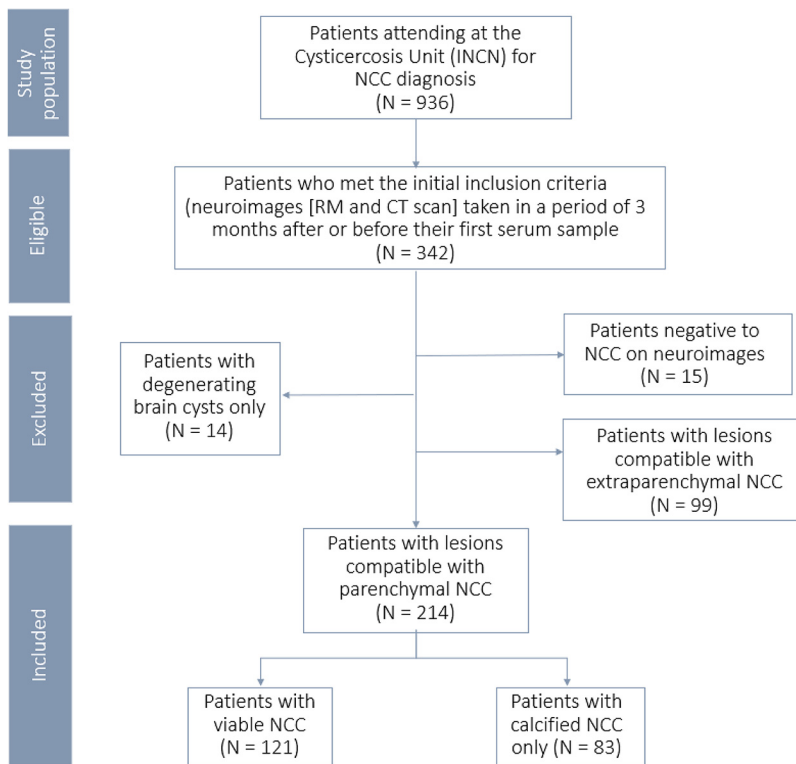
FIG 1 Flowchart of study population selection. RM, magnetic resonance.

either viable cysts (small, rounded fluid-filled lesions approximately 10 mm in diameter, hyperintense on T2 magnetic resonance imaging [MRI] sequences, with little or no pericystic edema, and in most cases with an internal nodule corresponding to the scolex [Fig. 2A]) or calcified lesions (nonenhancing hyperdense small nodule lesions seen on CT scan, with or without perilesional edema [Fig. 2B]) (2). Patients with lesions that upon review were not considered to be NCC were excluded, as well as patients with transitional or degenerating cysts only (nodular lesions with absence of liquid content signal and a marked perilesional inflammatory reaction) (33) as these lesions are not deemed as viable and are frequently negative in antigen testing (27), making them inappropriate for assessing the use of serology to detect viable NCC. Patients with extraparenchymal NCC, with either subarachnoid or ventricular cysts, were also excluded (due to their extremely strong serological response seen on EITB and Ag-ELISA).

Study procedures. (i) Images. Brain MRI and CT scan readings were performed by an independent neuroradiologist and reviewed by neurologists of the study team. Cases were classified as viable NCC (at least one viable cyst, with or without calcified lesions) or calcified NCC (presence of calcified lesions only), based on neuroimages. Cyst burden in cases with viable NCC was also recorded and classified as 1 to 2 cysts and 3 or more cysts.

(ii) EITB. The enzyme-linked immunoelectrotransfer blot (EITB) assay was processed as previously described by Tsang et al. (23). Banding pattern readings were performed by the laboratory technician and confirmed by a supervisor. Readers were blind to neuroimaging findings. Samples with doubtful responses (those with nonspecific band reactions or with unclear signal at the level of diagnostic bands) were reprocessed. EITB results were reported as the number of reactive bands (0 to 7). In addition, values of 0 or 1, indicating the presence or absence of each of the seven bands on EITB were also recorded.

(iii) Ag-ELISA. Antigen detection was performed using the B158/B60 MAb-based Ag-ELISA as previously described (25, 32). Optical density (OD) values were obtained and divided by the OD values from a pool of known negative samples for calculation of antigen ratios. Samples were considered positive if antigen ratios were equal to or greater than 1.

Statistical analysis. Radiological, serological, and demographic information of patients was described using summary statistics. Latent class analysis used dichotomous results (presence/absence) of each of the seven EITB antibody bands to group banding patterns into homogenous classes using maximum likelihood estimation methods. We ran models with 2 to 6 classes and defined the best-fitted model according to a statistical approach (using Akaike and Bayesian information criteria) and identification of representative banding pattern profiles between classes. Class prevalences and conditional class membership probabilities for each band were evaluated to confirm model structure. Bivariate associations between classes and patients' characteristics (imaging findings, Ag-ELISA results, antigen ratios, age, and sex) were performed. We assessed the effects of adding Ag-ELISA results to EITB class responses to predict or rule out viable NCC by comparing true-positive and false-negative Ag-ELISA results in each class using Fisher's exact test. CNS cyst burdens according to EITB class responses in patients positive and negative on Ag-ELISA were also evaluated using
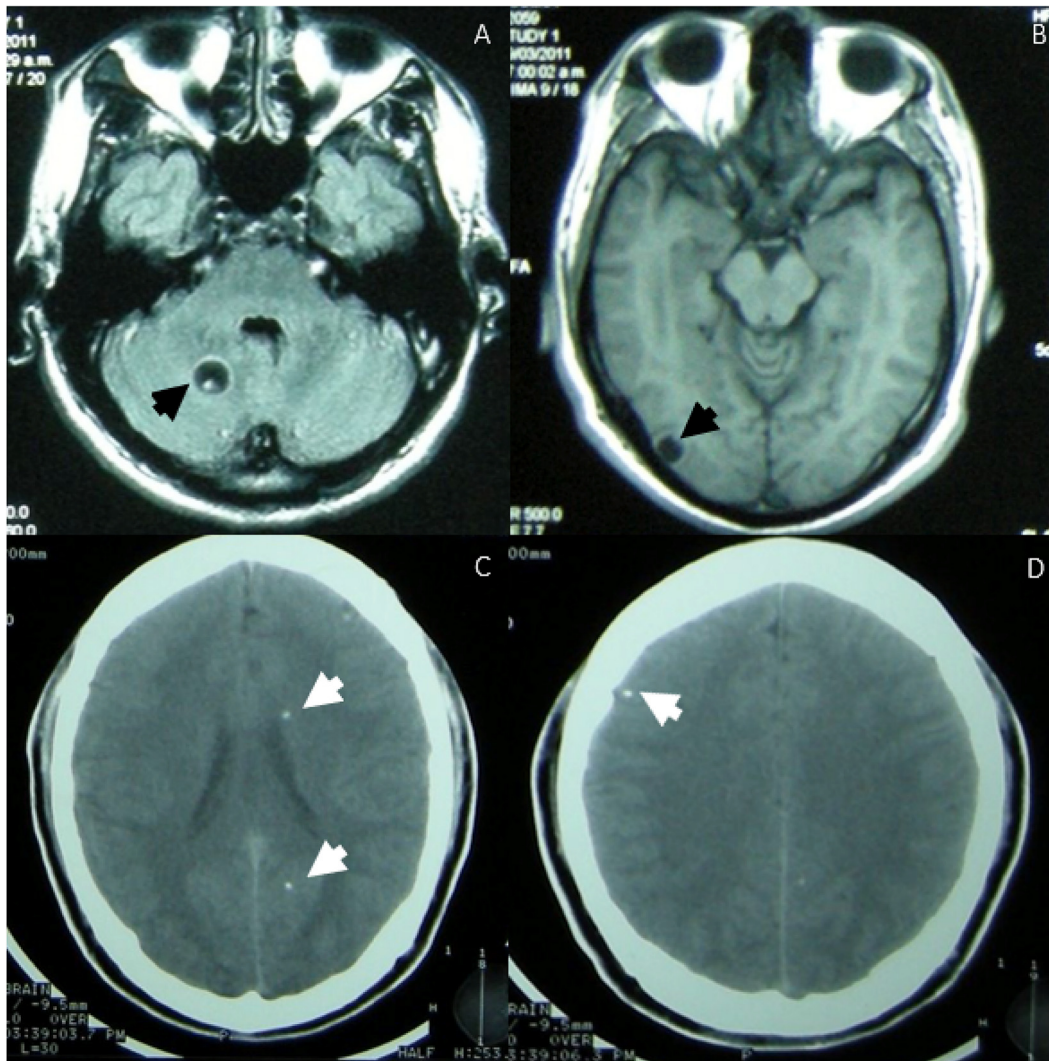
FIG 2 Neuroimages showing the characteristics of CNS cyst infection in a patient with parenchymal NCC. (A and B) Black arrows indicate viable cysts visualized using brain magnetic resonance imaging (MRI). (C and D) White arrows indicate calcified lesions on a computed tomography (CT) scan.

Cuzick's test for trend. Statistical analyses were carried out in RStudio v1.2.5001 using the package PoLCA for latent class models. Statistical significance was set to 5%.

Ethics. All study procedures described here were reviewed and approved by the institutional ethics review boards of Universidad Peruana Cayetano Heredia (IRB approval no. 103656) and Instituto Nacional de Ciencias Neurológicas (IRB approval no. 592-2019). All study participants signed an informed consent authorizing the use of their information.

RESULTS

A flowchart of the study population selection is shown in Fig. 1. During the period 2015 to 2019, a total of 936 symptomatic patients attended the Cysticercosis Unit at INCN for initial diagnosis of NCC, of which 342 met the initial criteria for eligibility. Subsequently, we excluded 15 patients with lesions that upon review were not deemed to be NCC, 4 patients with degenerating cysts only, and 99 patients with lesions compatible with extraparenchymal NCC. Thus, 214 patients with parenchymal NCC were included (median number of cysts, 2 [range, 0 to 114]; median number of calcifications, 2, [range, 0 to 99]); 131 had viable NCC, of which 72 (55%) had 3 or more cysts and 59 (45%) had 1 to 2 cysts. Eighty-three patients (38.8%) had calcified NCC only. Study participants had an average age of 43.2 ± 14.4 years, and 108 (50.5%) were female. A total of 183 patients (85.5%) were EITB positive (median number of bands, 4 [range, 0 to 7]), of which, almost all reacted

TABLE 1 Class description and distribution of EITB banding patterns in each class

Class description	n	No. of reactive bands	Banding pattern[a]	n (%)
Class 1: EITB negative or only positive to antigens of GP50 family	40	0	0000000	31 (77.5)
		1	1000000	9 (22.5)
Class 2: positive to antigens of T24/42 family, with or without reaction to GP50 antigens	62	2	0110000	12 (19.4)
		2	1010000	1 (1.6)
		2	1100000	3 (4.8)
		3	1110000	47 (74.2)
Class 3: positive to antigens of GP50 and T24/42 families and positive to antigens of 8-kDa family (GP21 and GP18 not together)	39	4	1110001	16 (41.0)
		4	1110010	4 (10.3)
		5	1110011	8 (20.5)
		5	1110101	3 (7.7)
		6	1110111	2 (5.1)
		5	1111001	3 (7.7)
		6	1111011	3 (7.7)
Class 4: positive to antigens of GP50 and T24/42 families and strongly positive to antigens of 8-kDa family (GP21 and GP18 together)	73	5	1111100	1 (1.4)
		6	1111101	3 (4.1)
		6	1111110	3 (4.1)
		7	1111111	66 (90.4)

[a]Values of 1 and 0 indicate the presence or absence of each of the EITB antibody bands (GP50, GP42-39, GP24, GP21, GP18, GP14, and GP13).

to the heavier glycoprotein antigens (GP50, 93.4%; GP42-39, 94.5%; GP24, 93.4%), while fewer reacted to low-molecular-weight glycoprotein antigens (GP21, 43.2%; GP18, 42.6%; GP14, 47%; GP13, 56.8%). Ag-ELISA was positive in 126 cases (58.9%; median Ag ratio, 2.2 [range, 0.2 to 124.1]) (see Table S1 in the supplemental material).

A total of 17 EITB banding patterns were identified for latent class analysis (Table 1). We found discrepancies for fit criteria using Akaike and Bayesian information criteria in latent class analysis. (The Akaike information criterion pointed to a 4-class model as optimal, whereas the Bayesian information criterion pointed to a 3-class model as optimal [see Table S2 in the supplemental material].) However, we decided to retain the 4-class model as it provided the strongest theoretical distinction between classes (identification of banding pattern profiles representative of the *T. solium* antigen families in each class, not observed in the 3-class model). Class 1 (*n* = 40, with 0 to 1 reactive band) included patients EITB negative or positive to the band GP50 alone (related to the GP50 antigen family). Class 2 (*n* = 62, with 2 to 3 reactive bands) included patients positive to GP42-39 and/or GP24 (related to the T24/42 antigen family), with or without reaction to GP50. Classes 3 (*n* = 39, with 4 to 6 reactive bands) and 4 (*n* = 73, with 5 to 7 reactive bands) included patients positive to GP50, GP42-39, and GP24 (GP50 and T24/42 antigen families) and reacting to antigens of the 8-kDa family (GP21, GP18, GP14, and GP13) (Fig. 3). Classes 3 and 4 differed both in the number of reacting bands (stronger responses in class 4 compared to class 3), and in the pattern of bands as well (bands GP21 and GP18 together in class 4, but not in class 3). Parameters derived from the latent class model (class prevalences and conditional class membership probabilities for each band) are shown in Table S3 in the supplemental material.

The distribution of patients with viable and calcified NCC varied between classes (Table 2). Most cases in classes 3 and 4 had viable NCC (32/39 [82.1%] and 64/73 [87.7%], respectively) compared to class 2 (33/62 [53.2%]), whereas in class 1, almost all patients had calcified NCC (38/40 [95.0%]) and only two cases had viable NCC. CNS cyst burden was also higher in classes 3 and 4 (median numbers of cysts, 3 [range, 0 to 56] and 3 [range:0 to 114], respectively) compared to class 2 (median number of cysts, 2 [range, 0 to 38]), whereas the two viable NCC cases in class 1 had one and two cysts, respectively. The distribution of patients positive on Ag-ELISA also differed between EITB class responses; 4/40 patients (10.0%) in class 1 were Ag-ELISA positive compared

FIG 3 Distribution of EITB banding patterns according to class membership. Classes: 1, EITB negative or only positive to antigens of the GP50 family (0 to 1 reactive band); 2, positive to antigens of the T24/42 family, with or without reaction to GP50 antigens (2 to 3 reactive bands); 3, positive to antigens of the GP50 and T24/42 families and positive to antigens of the 8-kDa family (4 to 6 reactive bands); 4, positive to antigens of the GP50 and T24/42 families and strongly positive to antigens of the 8-kDa family (5 to 7 reactive bands).

to 22/62 (35.5%) in class 2, and the numbers were much higher in classes 3 and 4 (33/39 [84.6%] and 67/73 [91.8%], respectively; $P < 0.001$). Antigen ratios were also statistically different between classes (higher in classes 3 and 4 and lower in classes 1 and 2) (Table 2). Age distribution followed a non-statistically significant trend, with lower age in stronger classes (3 and 4), while sex distribution did not differ between classes.

In class 2, the addition of Ag-ELISA results significantly improved discrimination of viable from nonviable NCC ($P < 0.001$); all 22 patients (100%) positive on Ag-ELISA in this class had viable NCC, whereas 11/40 patients (27.5%) negative on Ag-ELISA had viable NCC (1/13 [7.7%] reacted to 2 bands, and 10/27 [37.0%] reacted to 3 bands) (Table 3). Only 1 out of 4 patients positive on Ag-ELISA in class 1 had viable NCC, whereas 1/36 patients (2.8%) negative on Ag-ELISA had viable NCC ($P = 0.192$). Most cases positive on Ag-ELISA in classes 3 and 4 had viable NCC (29/33 [87.2%] and 58/67 [86.6%]), very similar to those observed in classes 3 and 4 alone, whereas 3 out of 6 cases (class 3) and all 6 cases (class 4) who were negative on Ag-ELISA had viable NCC.

CNS cyst burden according to EITB class responses and Ag-ELISA results is shown in Table S4 in the supplemental material. A higher proportion of patients positive on Ag-ELISA in classes 3 and 4 had 3 or more CNS cysts (20/33 [60.6%] and 40/67 [59.7%], respectively) compared to class 2 (10/22 [45.5%]) and class 1 (no cases with 3 or more cysts; P for trend, 0.073). Conversely, most patients negative on Ag-ELISA in classes 1 and 2 had calcified NCC or had few viable cysts (1 to 2), whereas in classes 3 and 4, most cases negative on Ag-ELISA had 1 to 2 viable cysts (2 out of 6 [33.3%] and 5 out of 6 [83.3%]; P for trend, <0.001).

DISCUSSION

Antiparasitic treatment in NCC accelerates the process of cyst destruction and resolution, decreasing the likelihood of further seizure episodes (14, 16). Neuroimaging is the main diagnostic tool in clinical settings for discrimination of viable and nonviable cyst infections in human parenchymal NCC, the latter not requiring antiparasitic treatment. Nonetheless, diagnosis of viable cysts by neuroimaging is not absolute and needs to be complemented by serology (33). Adding Ag-ELISA results to EITB banding

TABLE 2 Patients' characteristics according to EITB banding pattern classes

Characteristic	Result for[a]:				P
	Class 1 (n = 40)	Class 2 (n = 62)	Class 3 (n = 39)	Class 4 (n = 73)	
Age, mean ± SD yr	47.2 ± 15.5	43.4 ± 16.8	41.7 ± 12.0	41.8 ± 12.6	0.230
Sex, n (%)					0.100
Female	26 (65.0)	33 (53.2)	15 (38.5)	34 (46.6)	
Male	14 (35.0)	29 (46.8)	24 (61.5)	39 (53.4)	
Ag-ELISA					
Positive, n (%)	4 (10.0)	22 (35.5)	33 (84.6)	65 (89.0)	<0.001
Antigen ratio, median (range)	0.6 (0.2–20.7)	0.7 (0.2–23.4)	13.9 (0.2–89.0)	20.9 (0.4–124.1)	<0.001
Imaging findings					<0.001
Viable NCC	2 (5.0)	33 (53.2)	32 (82.1)	64 (87.7)	
Calcified NCC	38 (95.0)	29 (46.8)	7 (17.9)	9 (12.3)	
No. of viable cysts, median (range)	0 (0–2)	2 (0–38)	3 (0–56)	3 (0–114)	<0.001

[a]Classes: 1, negative or only positive to antigens of the GP50 family (0 to 1 reactive band); 2, positive to antigens of the T24/42 family, with or without reaction to GP50 antigens (2 to 3 reactive bands); 3, positive to antigens of the GP50 and T24/42 families and positive to antigens of the 8-kDa family (4 to 6 reactive bands); 4, positive to antigens of the GP50 and T24/42 families and strongly positive to antigens of the 8-kDa family (5 to 7 reactive bands).

patterns improves the ability to predict or rule out viable NCC, and their combined use may complement more accurately neuroimaging for a correct diagnosis.

Diagnosis of NCC requires correlation of serological results with neuroimaging to define infection characteristics (27, 31). The pattern of antibody responses is informative; responses in patients with NCC are heterogeneous and frequently involve multiple reactive bands (27,

TABLE 3 Distribution of patients with viable NCC according to EITB banding pattern classes and Ag-ELISA results

No. of reactive bands[a]	No. (%) of patients with viable NCC			
	Total (n = 214)	Ag-ELISA		P
		Positive (n = 126)	Negative (n = 88)	
Total	131/214 (61.2)	110/126 (87.3)	21/88 (23.9)	<0.001
Class 1				
0	1/31 (3.2)	0/2 (0.0)	1/29 (3.5)	0.935
1	1/9 (11.1)	1/2 (50.0)	0/7 (0.0)	0.222
Total	2/40 (5.0)	1/4 (25.0)	1/36 (2.8)	0.192
Class 2				
2	4/16 (25.0)	3/3 (100.0)	1/13 (7.7)	0.007
3	29/46 (63.0)	19/19 (100.0)	10/27 (37.0)	<0.001
Total	33/62 (53.2)	22/22 (100.0)	11/40 (27.5)	<0.001
Class 3				
4	14/20 (70.0)	12/16 (75.0)	2/4 (50.0)	0.549
5	13/14 (92.9)	12/12 (100.0)	1/2 (50.0)	0.143
6	5/5 (100.0)	5/5 (100.0)		
Total	32/39 (82.1)	29/33 (87.9)	3/6 (50.0)	0.059
Class 4				
5	1/1 (100.0)		1/1 (100.0)	
6	5/6 (83.3)	4/5 (80.0)	1/1 (100.0)	0.833
7	58/66 (87.9)	54/62 (87.1)	4/4 (100.0)	0.589
Total	64/73 (87.7)	58/67 (86.6)	6/6 (100.0)	0.440

[a]Classes: 1, EITB negative or only positive to antigens of the GP50 family (0 to 1 reactive band); 2, positive to antigens of the T24/42 family, with or without reaction to GP50 antigens (2 to 3 reactive bands); 3, positive to antigens of GP50 and T24/42 families and positive to antigens of the 8-kDa family (4 to 6 reactive bands); 4, positive to antigens of the GP50 and T24/42 families and strongly positive to antigens of the 8-kDa family (5 to 7 reactive bands).

in comparison with the weaker antibody responses observed in the general population (26, 34). The seven glycoprotein *T. solium* antigens in the EITB fall into three protein families—GP50, T24/42, and 8 kDa—which differ in structure and function (28–30). We previously showed that EITB banding patterns may be grouped in classes using latent class analysis, reflecting the distribution of antigen families (26). Here, we obtained similar classes for EITB antibody banding patterns, with class 1 including negative or weak antibody responses (GP50 alone) (28), class 2 including antibody responses to bands GP42-39 and GP24 (T24/42 antigen family) (29), and classes 3 and 4 including responses to low-weight bands (GP21, GP18, GP14 and GP13, 8-kDa family) (30), with more reactive antibody bands observed in class 4. Although classes 3 and 4 are similar in structure, their inclusion as distinct classes allowed the interpretation of the remaining classes in the model.

The proportions of participants with viable and calcified NCC differed between classes. Most cases in class 1 had calcified lesions only, since antibodies against GP50 persist longer after parasite death and resolution (27). Previous studies have also reported the poor predictive value of GP50 alone to detect viable NCC (26, 35). Class 2 included a mix of viable and calcified NCC cases. Most cases with viable NCC (>80%) and with high cyst burden were observed in classes 3 and 4. These distributions correlate well with the nature and probable function of each antigen family (26–30).

The effect of adding Ag-ELISA results to class 2 EITB patterns improved diagnostic ability to discriminate viable CNS infections. In this class, the probability of viable NCC in an Ag-ELISA-positive patient was 100%, almost double that for class 2 antibody results alone (53.2%). The GP42-39 and GP24 bands involve T24/42 family antigens (29), whereas the low-weight glycoprotein bands react to the more predictive 8-kDa antigen family. Nonetheless, 8-kDa may also be present in the positions of the higher-molecular-weight bands (GP24 and GP42-39), even if there is no detectable reaction in the smaller antigen bands (GP21, GP18, GP14, and GP13) (26, 30) Therefore, the addition of Ag-ELISA in class 2 responses may serve to identify the subgroup of patients in this class with 8-kDa antigens that could have viable NCC. On the other hand, the ability of a negative Ag-ELISA result to rule out viable NCC in class 2 was only moderate: 11/40 cases (27.5%) had viable NCC. These 11 cases with viable NCC, but negative on Ag-ELISA, harbored 1 to 2 cysts, which explains the false-negative Ag-ELISA results because of the assay's lower sensitivity in cases with few viable lesions (32).

In class 1, the effect of adding a positive Ag-ELISA result to predict viable NCC was limited by the small numbers of viable NCC cases (only two cases), as symptomatic cases with NCC are usually positive to more than one antibody band (27). Only 1 out 4 patients positive on Ag-ELISA in this class had viable NCC, corresponding to one case with a single viable cyst. On the other hand, while weak EITB responses are strongly associated with inactive CNS lesions (26), adding a negative Ag-ELISA result in class 1 may also serve to rule out viable NCC. (False-negative Ag-ELISA results in this class were low.)

In classes 3 and 4, the likelihood of viable NCC was very high in general and independently of adding a positive Ag-ELISA result. Also, a negative Ag-ELISA result in classes 3 and 4 was poorly predictive of inactive infection, as false-negative results of Ag-ELISA in these classes were high (50% and 100%). Most cases with viable NCC, but negative on Ag-ELISA, in classes 3 and 4 harbored 1 to 2 cysts, so these false-negative Ag-ELISA patients can be explained by the low sensitivity of antigen detection in few viable lesions (27, 31).

Some drawbacks in this study deserve to be considered. Our study included neuroimages and sera of patients with parenchymal NCC only, so our findings cannot be generalized to entire hospital-based populations. Nonetheless, we decided to include patients with parenchymal NCC as these cases represent the more frequent group of neurological cases in clinical settings. We excluded patients with degenerative lesions only because they were very few, and we are not certain about their viability, which may confound our assessment of viability of serological assays. It is also possible that some patients excluded from the study had unnoticed lesions on MRI and CT, which may result in selection bias for more visible infections. Also, we did not consider clinical information. The lack of adjustment by clinical covariates in latent class analysis did not seem to strongly affect our results as all cases with parenchymal NCC in our study were symptomatic, independent of their serological responses.

The diagnosis of NCC is based on neuroimaging and confirmed by serological assays. Many times, neuroimaging findings in parenchymal NCC are not always definitive, and as such, there is a need to know the strengths and drawbacks of supporting serological assays. Our findings demonstrate that Ag-ELISA results add little to negative or weak EITB responses (where antigen is usually negative) or to strongly positive EITB results (where antigen is usually positive). However, in class 2 responses (reactions to two or three bands), there are both patients with viable infections and those with nonviable infections. In this subset (class 2), the addition of an Ag-ELISA result clearly helps to define individuals with viable NCC infections.

In summary, combining EITB banding patterns with antigen detection improves the ability to predict or exclude viable CNS infection, particularly in class 2 responses. These results together more appropriately complement neuroimaging for the diagnosis of viable NCC in hospital settings and may also serve in resource-poor settings, where neuroimaging is not available to identify patients with probable viable NCC for referral to hospitals for diagnostic confirmation with neuroimages and clinical management.

SUPPLEMENTAL MATERIAL

Supplemental material is available online only.

SUPPLEMENTAL FILE 1, PDF file, 0.1 MB.

REFERENCES

1. Coyle CM, Mahanty S, Zunt JR, Wallin MT, Cantey PT, White AC, Jr, O'Neal SE, Serpa JA, Southern PM, Wilkins P, McCarthy AE, Higgs ES, Nash TE. 2012. Neurocysticercosis: neglected but not forgotten. PLoS Negl Trop Dis 6:e1500. https://doi.org/10.1371/journal.pntd.0001500.
2. Garcia HH, Nash TE, Del Brutto OH. 2014. Clinical symptoms, diagnosis, and treatment of neurocysticercosis. Lancet Neurol 13:1202–1215. https://doi.org/10.1016/S1474-4422(14)70094-8.
3. Lightowlers MW, Donadeu M. 2017. Designing a minimal intervention strategy to control Taenia solium. Trends Parasitol 33:426–434. https://doi.org/10.1016/j.pt.2017.01.011.
4. Garcia HH, Cysticercosis Working Group in Peru. 2012. Neurocysticercosis in immigrant populations. J Travel Med 19:73–75. https://doi.org/10.1111/j.1708-8305.2011.00583.x.
5. O'Neal SE, Flecker RH. 2015. Hospitalization frequency and charges for neurocysticercosis, United States, 2003–2012. Emerg Infect Dis 21:969–976. https://doi.org/10.3201/eid2106.141324.
6. Nii-Trebi NI. 2017. Emerging and neglected infectious diseases: insights, advances, and challenges. Biomed Res Int 2017:5245021. https://doi.org/10.1155/2017/5245021.
7. Torgerson PR, Macpherson CN. 2011. The socioeconomic burden of parasitic zoonoses: global trends. Vet Parasitol 182:79–95. https://doi.org/10.1016/j.vetpar.2011.07.017.
8. Takayanagui OM, Odashima NS. 2006. Clinical aspects of neurocysticercosis. Parasitol Int 55(Suppl):S111–S115. https://doi.org/10.1016/j.parint.2005.11.016.
9. Carabin H, Ndimubanzi PC, Budke CM, Nguyen H, Qian Y, Cowan LD, Stoner JA, Rainwater E, Dickey M. 2011. Clinical manifestations associated

with neurocysticercosis: a systematic review. PLoS Negl Trop Dis 5:e1152. https://doi.org/10.1371/journal.pntd.0001152.

10. Debacq G, Moyano LM, Garcia HH, Boumediene F, Marin B, Ngoungou EB, Preux PM. 2017. Systematic review and meta-analysis estimating association of cysticercosis and neurocysticercosis with epilepsy. PLoS Negl Trop Dis 11:e0005153. https://doi.org/10.1371/journal.pntd.0005153.

11. Ndimubanzi PC, Carabin H, Budke CM, Nguyen H, Qian YJ, Rainwater E, Dickey M, Reynolds S, Stoner JA. 2010. A systematic review of the frequency of neurocyticercosis with a focus on people with epilepsy. PLoS Negl Trop Dis 4:e870. https://doi.org/10.1371/journal.pntd.0000870.

12. Nash T. 2012. Edema surrounding calcified intracranial cysticerci: clinical manifestations, natural history, and treatment. Pathog Glob Health 106: 275–279. https://doi.org/10.1179/2047773212Y.0000000026.

13. Nash TE, Mahanty S, Loeb JA, Theodore WH, Friedman A, Sander JW, Singh G, Cavalheiro E, Del Brutto OH, Takayanagui OM, Fleury A, Verastegui M, Preux PM, Montano S, Pretell EJ, White AC, Jr, Gonzales AE, Gilman RH, Garcia HH. 2015. Neurocysticercosis: a natural human model of epileptogenesis. Epilepsia 56:177–183. https://doi.org/10.1111/epi.12849.

14. Garcia HH, Pretell EJ, Gilman RH, Martinez SM, Moulton LH, Del Brutto OH, Herrera G, Evans CA, Gonzalez AE, Cysticercosis Working Group in Peru. 2004. A trial of antiparasitic treatment to reduce the rate of seizures due to cerebral cysticercosis. N Engl J Med 350:249–258. https://doi.org/10.1056/NEJMoa031294.

15. Garcia HH, Gonzales I, Lescano AG, Bustos JA, Zimic M, Escalante D, Saavedra H, Gavidia M, Rodriguez L, Najar E, Umeres H, Pretell EJ, Cysticercosis Working Group in Peru. 2014. Efficacy of combined antiparasitic therapy with praziquantel and albendazole for neurocysticercosis: a double-blind, randomised controlled trial. Lancet Infect Dis 14:687–695. https://doi.org/10.1016/S1473-3099(14)70779-0.

16. Garcia HH, Del Brutto OH, Cysticercosis Working Group in Peru. 2017. Antiparasitic treatment of neurocysticercosis—the effect of cyst destruction in seizure evolution. Epilepsy Behav 76:158–162. https://doi.org/10.1016/j.yebeh.2017.03.013.

17. Garcia HH, Del Brutto OH. 2003. Imaging findings in neurocysticercosis. Acta Trop 87:71–78. https://doi.org/10.1016/s0001-706x(03)00057-3.

18. del Brutto OH. 1997. Neurocysticercosis in children: clinical and radiological analysis and prognostic factors in 54 patients. Rev Neurol 25:1681–1684. (In Spanish.)

19. Teitelbaum GP, Otto RJ, Lin M, Watanabe AT, Stull MA, Manz HJ, Bradley WG, Jr. 1989. MR imaging of neurocysticercosis. AJR Am J Roentgenol 153: 857–866. https://doi.org/10.2214/ajr.153.4.857.

20. Martinez HR, Rangel-Guerra R, Elizondo G, Gonzalez J, Todd LE, Ancer J, Prakash SS. 1989. MR imaging in neurocysticercosis: a study of 56 cases. AJNR Am J Neuroradiol 10:1011–1019.

21. Del Brutto OH. 2014. Neurocysticercosis. Neurohospitalist 4:205–212. https://doi.org/10.1177/1941874414533351.

22. Del Brutto OH, Nash TE, White AC, Jr, Rajshekhar V, Wilkins PP, Singh G, Vasquez CM, Salgado P, Gilman RH, Garcia HH. 2017. Revised diagnostic criteria for neurocysticercosis. J Neurol Sci 372:202–210. https://doi.org/10.1016/j.jns.2016.11.045.

23. Tsang VC, Brand JA, Boyer AE. 1989. An enzyme-linked immunoelectrotransfer blot assay and glycoprotein antigens for diagnosing human cysticercosis (Taenia solium). J Infect Dis 159:50–59. https://doi.org/10.1093/infdis/159.1.50.

24. Wilson M, Bryan RT, Fried JA, Ware DA, Schantz PM, Pilcher JB, Tsang VC. 1991. Clinical evaluation of the cysticercosis enzyme-linked immunoelectrotransfer blot in patients with neurocysticercosis. J Infect Dis 164: 1007–1009. https://doi.org/10.1093/infdis/164.5.1007.

25. Zea-Vera A, Cordova EG, Rodriguez S, Gonzales I, Pretell EJ, Castillo Y, Castro-Suarez S, Gabriel S, Tsang VC, Dorny P, Garcia HH, Cysticercosis Working Group in Peru. 2013. Parasite antigen in serum predicts the presence of viable brain parasites in patients with apparently calcified cysticercosis only. Clin Infect Dis 57:e154–e159. https://doi.org/10.1093/cid/cit422.

26. Arroyo G, Rodriguez S, Lescano AG, Alroy KA, Bustos JA, Santivanez S, Gonzales I, Saavedra H, Pretell EJ, Gonzalez AE, Gilman RH, Tsang VCW, Garcia HH, Cysticercosis Working Group in Peru. 2018. Antibody banding patterns of the enzyme-linked immunoelectrotransfer blot and brain imaging findings in patients with neurocysticercosis. Clin Infect Dis 66: 282–288. https://doi.org/10.1093/cid/cix774.

27. Garcia HH, O'Neal SE, Noh J, Handali S, Cysticercosis Working Group in Peru. 2018. Laboratory diagnosis of neurocysticercosis (Taenia solium). J Clin Microbiol 56:e00424-18. https://doi.org/10.1128/JCM.00424-18.

28. Hancock K, Pattabhi S, Greene RM, Yushak ML, Williams F, Khan A, Priest JW, Levine MZ, Tsang VC. 2004. Characterization and cloning of GP50, a Taenia solium antigen diagnostic for cysticercosis. Mol Biochem Parasitol 133:115–124. https://doi.org/10.1016/j.molbiopara.2003.10.001.

29. Hancock K, Pattabhi S, Whitfield FW, Yushak ML, Lane WS, Garcia HH, Gonzalez AE, Gilman RH, Tsang VC. 2006. Characterization and cloning of T24, a Taenia solium antigen diagnostic for cysticercosis. Mol Biochem Parasitol 147:109–117. https://doi.org/10.1016/j.molbiopara.2006.02.004.

30. Hancock K, Khan A, Williams FB, Yushak ML, Pattabhi S, Noh J, Tsang VC. 2003. Characterization of the 8-kilodalton antigens of Taenia solium metacestodes and evaluation of their use in an enzyme-linked immunosorbent assay for serodiagnosis. J Clin Microbiol 41:2577–2586. https://doi.org/10.1128/JCM.41.6.2577-2586.2003.

31. Rodriguez S, Wilkins P, Dorny P. 2012. Immunological and molecular diagnosis of cysticercosis. Pathog Glob Health 106:286–298. https://doi.org/10.1179/2047773212Y.0000000048.

32. Rodriguez S, Dorny P, Tsang VC, Pretell EJ, Brandt J, Lescano AG, Gonzalez AE, Gilman RH, Garcia HH, Cysticercosis Working Group in Peru. 2009. Detection of Taenia solium antigens and anti-T. solium antibodies in paired serum and cerebrospinal fluid samples from patients with intraparenchymal or extraparenchymal neurocysticercosis. J Infect Dis 199:1345–1352. https://doi.org/10.1086/597757.

33. Garcia HH, Gonzalez AE, Gilman RH. 2020. Taenia solium cysticercosis and its impact in neurological disease. Clin Microbiol Rev 33:e00085-19. https://doi.org/10.1128/CMR.00085-19.

34. Moyano LM, O'Neal SE, Ayvar V, Gonzalvez G, Gamboa R, Vilchez P, Rodriguez S, Reistetter J, Tsang VC, Gilman RH, Gonzalez AE, Garcia HH, Cysticercosis Working Group in Peru. 2016. High prevalence of asymptomatic neurocysticercosis in an endemic rural community in Peru. PLoS Negl Trop Dis 10:e0005130. https://doi.org/10.1371/journal.pntd.0005130.

35. Furrows SJ, McCroddan J, Bligh WJ, Chiodini P. 2006. Lack of specificity of a single positive 50-kDa band in the electroimmunotransfer blot (EITB) assay for cysticercosis. Clin Microbiol Infect 12:459–462. https://doi.org/10.1111/j.1469-0691.2006.01381.x.